Beyond Marchenko
Obtaining virtual receivers and virtual sources in the subsurface

Singh, Satyan; Wapenaar, Kees; van der Neut, Joost; Snieder, R

DOI
10.1190/segam2016-13964312.1

Publication date
2016

Document Version
Accepted author manuscript

Published in
SEG Technical Program Expanded Abstracts 2016

Citation (APA)
Singh, S., Wapenaar, K., van der Neut, J., & Snieder, R. (2016). Beyond Marchenko: Obtaining virtual receivers and virtual sources in the subsurface. In C. Sicking, & J. Ferguson (Eds.), *SEG Technical Program Expanded Abstracts 2016* (pp. 5166-5171). (SEG Technical Program Expanded Abstracts; Vol. 2016). SEG. https://doi.org/10.1190/segam2016-13964312.1

Beyond Marchenko – Obtaining virtual receivers and virtual sources in the subsurface

S. Singh[1], *J. van der Neut*[2], *K. Wapenaar*[2], *R. Snieder*[1]
(1) Center for Wave Phenomena, Department of Geophysics, Colorado School of Mines, Golden, Colorado, USA
(2) Department of Geoscience and Engineering, Delft University of Technology, GA Delft, The Netherlands

SUMMARY

By solving the Marchenko equations, the Green's function can be retrieved between a virtual receiver in the subsurface to points at the *surface* (no physical receiver is required at the virtual location). We extend the idea of these equations to retrieve the Green's function between any two points in the *subsurface*; i.e, between a virtual source and a virtual receiver (no physical source or physical receiver is required at either of these locations). This Green's function is called the virtual Green's function and includes all the primaries, internal and free-surface multiples. Similar to the Marchenko Green's function, we require the reflection response at the surface (single-sided illumination) and an estimate of the first arrival travel time from the virtual location to the surface.

INTRODUCTION

We propose a method to retrieve the Green's function between two points in the subsurface of the Earth. We call these two points a virtual source and a virtual receiver pair. To retrieve the Green's function at a virtual receiver for a virtual source we require neither a physical source nor a physical receiver at the virtual source and receiver. The requirements for the retrieval of this Green's function is the reflection response for physical sources and physical receivers at the surface (single sided-illumination) and a smooth version of the velocity model (no small-scale details of the model are necessary). For brevity we define this Green's function i.e., the response of a virtual source recorded at a virtual receiver, as the *Virtual Green's function*. We label the method of retrieving the *Virtual Green's function* as the modified Marchenko method.

Similar ideas of retrieving the Green's function between two points have been proposed in seismic interferometry (Wapenaar, 2004; Curtis et al., 2006; Snieder et al., 2007; Bakulin and Calvert, 2006; van Manen et al., 2006; Curtis et al., 2009; Curtis and Halliday, 2010) and in the Marchenko method (Broggini et al., 2012; Broggini and Snieder, 2012; Wapenaar et al., 2013; Slob et al., 2014; Wapenaar et al., 2014; Singh et al., 2015, 2016). However, these methods (interferometry and Marchenko method) have more restrictions in the source-receiver geometry, as discussed later, for the accurate retrieval of the Green's function than our proposed method (modified Marchenko method).

In seismic interferometry, we create virtual sources at locations where there are physical receivers. We also require a closed surface of sources to adequately retrieve the Green's function. Unlike interferometry, a physical receiver or physical source is not needed by our modified Marchenko method to create either a virtual source or a virtual receiver and we only require single-sided illumination (a closed surface of sources not needed). The Green's function retrieved by the Marchenko equations is the response to a virtual source in the subsurface recorded at **physical receivers** at the **surface** (Broggini et al., 2012; Broggini and Snieder, 2012; Wapenaar et al., 2013; Slob et al., 2014; Wapenaar et al., 2014; Singh et al., 2015, 2016). The Marchenko retrieved Green's function requires neither a physical source nor a physical receiver at the virtual source location in the subsurface.

Our algorithm retrieves the Green's function (both up- and down-going at the receiver) for virtual sources and virtual receivers. The Marchenko-retrieved Green's functions are limited to virtual sources in the subsurface recorded at the **surface** but the Modified Marchenko method (our Work) is not restricted to recording on the surface for each virtual source. In our method, the response of the virtual source can be retrieved for a virtual reciever anywhere in the **subsurface**.

Wapenaar et al. (2016) has proposed similar work to ours, but their approach retrieves (1) the two-way virtual Green's function while our work retrieves the up- and down- going (one-way) virtual Green's function, the summation of these one-way Green's function gives the two-way Green's function, and (2) the homogeneous Green's function while we retrieve the causal Green's function.

We discuss in this paper the theory of retrieving the virtual Green's function. Our numerical examples are split into two sections (1) A verification of our algorithm in 1D (2) A 2D numerical example of the virtual Green's function constructed in such a way that we create a wavefield with all the reflections and first arrivals from a virtual source. This last numerical example is complicated since the discontinuities in the density and the velocity are at different locations.

THEORY

To retrieve the Green's function from a virtual receiver in the subsurface for *sources on the surface*, one solves the Marchenko equations. The retrieval only requires the reflection response at the surface and an estimate of the first arrival travel-time from the virtual receiver to the surface. The retrieved Green's function can either include free-surface multiples (Singh et al., 2015, 2016) or exclude these multiples (Broggini et al., 2012; Broggini and Snieder, 2012; Wapenaar et al., 2013; Slob et al., 2014; Wapenaar et al., 2014). In addition to the retrieved Green's function, the Marchenko equations also give us the one-way focusing functions. These functions are outputs from the Marchenko equations that exist at the acquisition level ∂D_0 (acquisition surface) and focus on an arbitrary depth level ∂D_i at $t = 0$ (time equal zero).

	State A	State B
On ∂D_0:	$p_A^+ = f_1^+(\mathbf{x_0}, \mathbf{x_i'}, \omega)$	$p_B^+ = rG^-(\mathbf{x_0}, \mathbf{x_j''}, \omega)$
	$p_A^- = f_1^-(\mathbf{x_0}, \mathbf{x_i'}, \omega)$	$p_B^- = G^-(\mathbf{x_0}, \mathbf{x_j''}, \omega)$
On ∂D_i:	$p_A^+ = f_1^+(\mathbf{x_i}, \mathbf{x_i'}, \omega) = \delta(\mathbf{x}_H - \mathbf{x}_H')$	$p_B^+ = G^+(\mathbf{x_i}, \mathbf{x_j''}, \omega)$
	$p_A^- = f_1^-(\mathbf{x_i}, \mathbf{x_i'}, \omega) = 0$	$p_B^- = G^-(\mathbf{x_i}, \mathbf{x_j''}, \omega)$

Table 1: The wavefields of the focusing function f_1 and Green's functions at the acquisition surface ∂D_0 and the level ∂D_i. $p_A^{\pm}$ symbolizes one-way wavefields in the frequency domain for wave state A, at arbitrary depth levels in the reference medium while $p_B^{\pm}$ symbolizes one-way wavefields at arbitrary depth levels in the inhomogeneous medium in wave state B, where r is the reflection coefficient of the free surface.

The focusing functions are auxiliary wavefields that reside in a truncated medium that has the same material properties as the actual inhomogeneous medium between ∂D_0 and ∂D_i and that is homogeneous above ∂D_0 and reflection-free below ∂D_i (Slob et al., 2014). Therefore, the boundary conditions on ∂D_0 and ∂D_i in the truncated medium, where the focusing function exists, are reflection-free. Our algorithm moves the sources of the Green's function retrieved by Marchenko equations from the surface into the subsurface at a virtual point with the help of the focusing function.

In this paper, the spatial coordinates are defined by their horizontal and depth components; for instance $\mathbf{x_0} = (\mathbf{x_{H,0}}, x_{3,0})$, where $\mathbf{x_{H,0}}$ stands for the horizontal coordinates at a depth $x_{3,0}$. Superscript $(+)$ refers to down-going waves and $(-)$ to up-going waves at the observation point $\mathbf{x}$. Additionally, wavefield quantities with a subscript 0 (e.g., R_0) indicates that no free-surface is present. One-way reciprocity theorems of the convolution and correlation type are used to relate up- and down-going fields at arbitrary depth levels to each other in different wave states (Wapenaar and Grimbergen, 1996).

The correlation reciprocity theorem is based on time reversal invariance of our wavefields, which implicitly assumes that the medium is lossless. Since we assume the wavefields can be decomposed into up- and down-going waves, we ignore evanescent waves.

Wave state A is defined for the truncated medium where the focusing functions reside. The one-way wavefields for wave state A that focus at $\mathbf{x_i'}$ (above $\mathbf{x_j''}$) are given in Table 1.

The Green's functions in the actual medium are defined as wave state B. The one-way wavefields for wave state B, the actual medium, for a source at $\mathbf{x_j''}$ are given in Table 1. We substitute the one-way wavefields described in Table 1 into the reciprocity theorems and use the sifting property of the delta function to yield

$$G^-(\mathbf{x_i'}, \mathbf{x_j''}, \omega) = \int_{-\infty}^{\infty} [G^-(\mathbf{x_0}, \mathbf{x_j''}, \omega) f_1^+(\mathbf{x_0}, \mathbf{x_i'}, \omega) - rG^-(\mathbf{x_0}, \mathbf{x_j''}, \omega) f_1^-(\mathbf{x_0}, \mathbf{x_i'}, \omega)] d\mathbf{x_0}, \quad (1)$$

$$G^+(\mathbf{x_i'}, \mathbf{x_j''}, \omega)^* = \int_{-\infty}^{\infty} [rG^-(\mathbf{x_0}, \mathbf{x_j''}, \omega)^* f^+(\mathbf{x_0}, \mathbf{x_i'}, \omega) - G^-(\mathbf{x_0}, \mathbf{x_j''}, \omega)^* f^-(\mathbf{x_0}, \mathbf{x_i'}, \omega)] d\mathbf{x_0}, \quad (2)$$

where r denotes the reflection coefficient of the free surface (in the examples shown in this paper $r = -1$.)

Equations 1 and 2 yield the up- and down-going virtual Green's functions, respectively, for a virtual receiver at $\mathbf{x_i'}$ and a virtual source at $\mathbf{x_j''}$ in the subsurface. Note that for the total Green's function, we are not limited to the source $\mathbf{x_j''}$ being below the receiver $\mathbf{x_i'}$ since by reciprocity, $G(\mathbf{x_i'}, \mathbf{x_j''}, t) = G(\mathbf{x_j''}, \mathbf{x_i'}, t)$. To compute the up- and down-going virtual Green's function in equations 1 and 2, we require 1) the Green's function $G^-(\mathbf{x_0}, \mathbf{x_j''}, \omega)$ at the surface $\mathbf{x_0}$ for a focal point at $\mathbf{x_j''}$ and 2) the focusing function $f^{\pm}(\mathbf{x_0}, \mathbf{x_i'}, \omega)$ at the surface $\mathbf{x_0}$ for a virtual source at $\mathbf{x_i'}$. We retrieve both these functions by solving the Marchenko equations which requires the reflection response (including free-surface multiples) as input (Singh et al., 2015, 2016). Note that these Green's functions $G^-(\mathbf{x_0}, \mathbf{x_j''}, \omega)$ include the primary, internal, and free-surface multiple reflections of the actual medium.

We can also retrieve the virtual Green's function which does not include free-surface multiples by simply setting the reflection coefficient at the free-surface r to zero in equations 1 and 2. Thus, the equation to retrieve the virtual Green's function without the presence of a free surface is

$$G_0^-(\mathbf{x_i'}, \mathbf{x_j''}, \omega) = \int_{-\infty}^{\infty} G_0^-(\mathbf{x_0}, \mathbf{x_j''}, \omega) f^+(\mathbf{x_0}, \mathbf{x_i'}, \omega) d\mathbf{x_0}, \quad (3)$$

$$G_0^+(\mathbf{x_i'}, \mathbf{x_j''}, \omega)^* = -\int_{-\infty}^{\infty} G_0^-(\mathbf{x_0}, \mathbf{x_j''}, \omega)^* f^-(\mathbf{x_0}, \mathbf{x_i'}, \omega) d\mathbf{x_0}, \quad (4)$$

where $G_0^{\pm}(\mathbf{x_i'}, \mathbf{x_j''}, \omega)$ is the up- and down-going Green's function without free-surface multiples for a virtual receiver at $\mathbf{x_i'}$ and virtual source at $\mathbf{x_j''}$.

NUMERICAL EXAMPLES

The first example illustrates the retrieval of the virtual Green's function with the free-surface reflections (Figure 1) for the 1D model given in Figure 2 with the virtual source and receiver shown by the blue and red dots, respectively. This example also contains variable density, with discontinuities at the same depth as the velocity model, with densities ranging from 1 $g\ cm^{-3}$ to 3 $g\ cm^{-3}$. As shown in Figure 1, there is an almost perfect match between the modeled Green's function and the retrieved virtual Green's function. The 1D numerical example have *perfect* aperture, hence, the 1D examples almost perfectly match the retrieved virtual Green's function to the modeled Green's function. Note that to retrieve the virtual Green's function in Figure 1 we only use the reflection response at the surface.

A fair question to ask is: why not use interferometry to cross-correlate the Green's function at a virtual receiver and at virtual source to get the virtual Green's function between the virtual source and the receiver? This interferometric method will not retrieve the virtual Green's function when we only have a

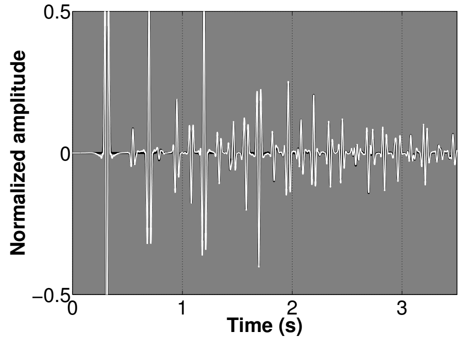

Figure 1: Virtual Green's function with free-surface multiples (white line) with virtual source $\mathbf{x}_\mathbf{j}''$ at depth 1.75 km and recording at the virtual receiver $\mathbf{x}_\mathbf{i}'$ at depth 0.75 km for the model in Figure 2 with a free surface. The modeled Green's function is superimposed on it which also includes the free-surface multiples (black line).

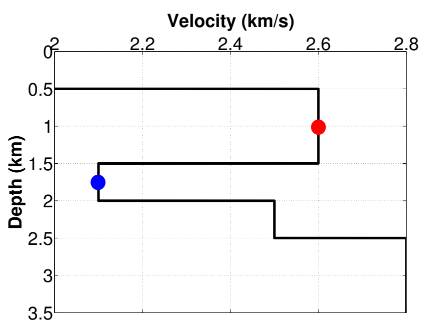

Figure 2: 1D velocity model with a free surface. The red dot at 0.75 km is the location of the virtual receiver while the blue dot at 1.75 km is the position of the virtual source for the retrieved virtual Green's function.

source at the surface because interferometry requires sources on both sides of the receiver. In Figure 3 (red line), we show the interferometric Green's function, (cross-correlation of the Green's functions from the virtual source and receiver to the surface), for the same model (see Figure 1) with the same virtual source $\mathbf{x}_\mathbf{j}'' = 1.75\ km$ and virtual receiver $\mathbf{x}_\mathbf{i}' = 0.75\ km$ locations in the 1D example. Since we have reflectors below the virtual source location $\mathbf{x}_\mathbf{j}'' = 1.75\ km$ (see Figure 2) and our physical sources are at the surface, our interferometric Green's function does not match the modeled or virtual Green's function (see Figure 3 – white line). This mis-match is caused by ignoring contributions from reflectors below the virtual source (we violated the requirement of the closed surface interferometric integral for physical sources that create the virtual source).

We next show a 2D numerical example of the virtual Green's function in a velocity and density model shown in Figures 4a and 4b, respectively. Notice that the discontinuities and the dip of the interfaces in the velocity are different from those in the density.

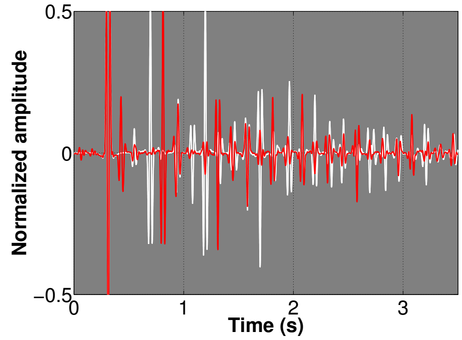

Figure 3: Virtual Green's function with virtual source $\mathbf{x}_\mathbf{j}''$ at depth 1.75 m and recording at the virtual receiver $\mathbf{x}_\mathbf{i}'$ at depth 0.75 km retrieved by the method of this paper (white line) and computed by interferometry (red line). The retrieved virtual Green's function (white line) is almost identical to the modeled virtual Green's function.

Our algorithm allows us to place virtual receivers and virtual sources in any target location in the subsurface. For our numerical example, we retrieve the virtual Green's function $G(\mathbf{x}_\mathbf{i}', \mathbf{x}_\mathbf{j}'', t)$, Figure 5, where $\mathbf{x}_\mathbf{i}'$ are the virtual receivers populating the target location at every 32 m (black box in Figure 4a) and $\mathbf{x}_\mathbf{j}'' = (0, 0.7)\ km$ is the virtual source (black dot in Figure 4a). In Figure 5 notice:

1. In panel b, the first arrival from the virtual source $\mathbf{x}_\mathbf{j}'' = (0, 0.7)\ km$ and the reflection from the bottom velocity layer.
2. In panels c and d, the inability of our algorithm to handle the horizontal propagating energy of the first arrival from the virtual source, hence the dimming on the sides of the first arrival of the virtual Green's function. To retrieve near-horizontally propagating events (in this case, these waves are not evanescent) especially in the first arrival of the virtual Green's function, we require a much larger aperture than is used in this example. Note that the later arriving up- and down-ward propagating waves are retrieved accurately at the depth of the virtual source $\mathbf{x}_\mathbf{j}'' = (0, 0.7)\ km$ in Figure 5, panel d and e, since the reflections are purely up- and down-going.
3. In panels c and d, we do however, retrieve the reflections from the density layer (pink line in Figure 5) although we did not use any explicit information of the density model in our numerical retrieval of the virtual Green's function.
4. In panel f, a free-surface multiple is present. As expected, there is a polarity change of the free surface multiple compared to the incident wave at the top of panel e due to the interaction of this wave in panel e with the free surface.
5. In panel h, we obtain the up-going reflections caused by the free-surface multiple interacting with the velocity and density layer.

In our algorithm, we evaluate an integral over space us-

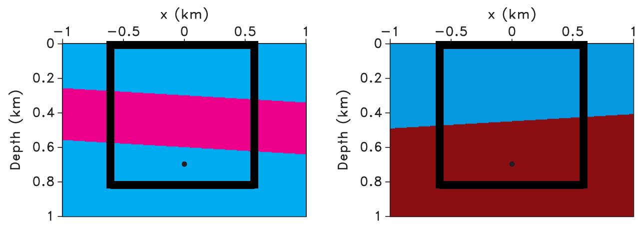

(a) (b)

Figure 4: Synthetic model (a) velocity model with velocities ranging from 2.0 to 2.4 km/s (b) one-interface density model with densities ranging from 2.0 to 3.0 g/cm^3 . The dot shows the position of the virtual source for the virtual Green's function and the black box is the target zone where we place virtual receivers.

ing a sampling interval dx, for example, in equations 1 and 2. These integrals over space, which include the stationary phase contribution, also generate artifacts due to end point contributions. Similar to interferometry, these artifacts can be mitigated through tapering at the edges of the integration interval (Mehta et al., 2008; van der Neut et al., 2009). In our 2D model these artifacts that arise from the integrals over space are also present. We remove these artifacts by muting the wavefield before the first arrival of the virtual source $\mathbf{x}''_\mathbf{j}$, and estimate the travel time of the first arrival using the smooth velocity model.

DISCUSSION

The theory of the virtual Green's function is based on Marchenko equations and uses the Marchenko solutions as well; hence, the virtual Green's function also suffers from the shortcomings and requirements of the Marchenko retrieved Green's function that are described elsewhere (Broggini et al., 2012; Broggini and Snieder, 2012; Wapenaar et al., 2013; Slob et al., 2014; Wapenaar et al., 2014; Singh et al., 2015, 2016).

For the simple 2D model, the discontinuities and dip in the velocity and density are different. However, we retrieve the two-way and one-way wavefield of the virtual Green's function without any knowledge of the density model and small-scale details in the velocity model. Figure 5 shows reflections from the density interface (middle interface in Figure 5), even though no density information was included in our algorithm. We retrieve these reflections because the density information is embedded in the reflection response recorded at the surface and the Marchenko equations are able to retrieve the density reflections from this response.

CONCLUSION

We can retrieve the Green's function between two points in the subsurface with single-sided illumination. Generally, interferometry gives inaccurate Green's functions for illumination from above (single-sided) because we do not have the illumination contributions from below. However, the Marchenko equations can be thought of as the mechanism to obviate the need for illumination from below to retrieve the virtual Green's function. The removal of the requirement for illumination from below (for interferometry) comes from the use of the focusing function, a solution to the Marchenko equations. The events in the focusing function only depend on the truncated medium and this function is solved using illumination only from above. In this paper, we explore this single-side illumination advantage of the focusing function to avoid the illumination from below to retrieve the virtual Green's function.

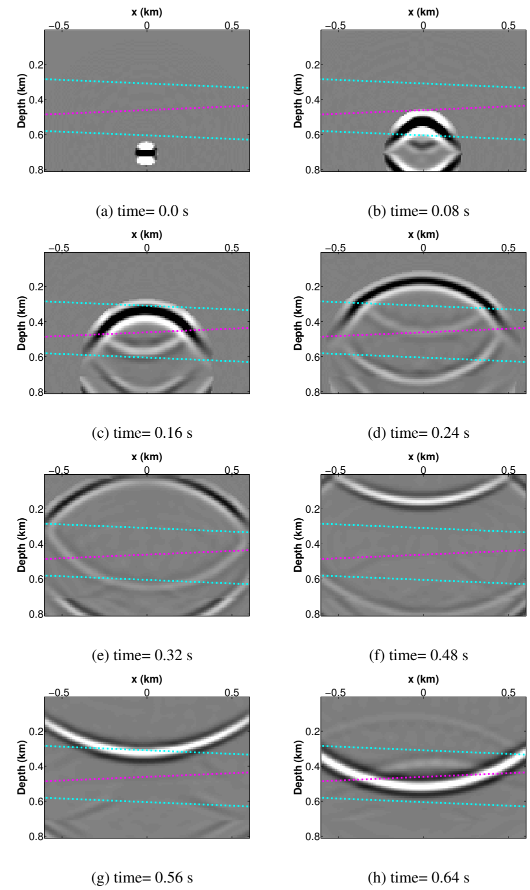

(a) time= 0.0 s (b) time= 0.08 s (c) time= 0.16 s (d) time= 0.24 s (e) time= 0.32 s (f) time= 0.48 s (g) time= 0.56 s (h) time= 0.64 s

Figure 5: Snapshots of the virtual Green's function $G(\mathbf{x}'_\mathbf{i}, \mathbf{x}''_\mathbf{j}, t)$ with virtual sources $\mathbf{x}''_\mathbf{j} = (0, 0.7)$ km and virtual receivers $\mathbf{x}'_\mathbf{i}$ populating the target box in Figure 4a. The dotted lines represent the velocity interface (blue) and the density interface (magenta).

Acknowledgments
We thank Ivan Vasconcelos (Schlumberger Gould Research) for fruitful discussions. This work was funded by the sponsor companies of the Consortium Project on Seismic Inverse Methods for Complex Structures and by Shell Research.